



Revista Mexicana de Física

ISSN: 0035-001X

rmf@ciencias.unam.mx

Sociedad Mexicana de Física A.C.

México

Vieira, M.; Fernandes, M.; Louro, P.; Fantoni, A.; Lavareda, G.; Carvalho, C.N.; Vygranenko, Y.

A real-time colour and image processing p-i-n/p-i-n device with optical readout

Revista Mexicana de Física, vol. 52, núm. 2, febrero, 2006, pp. 79-82

Sociedad Mexicana de Física A.C.

Distrito Federal, México

Available in: <http://www.redalyc.org/articulo.oa?id=57028295024>

- How to cite
- Complete issue
- More information about this article
- Journal's homepage in redalyc.org

redalyc.org

Scientific Information System

Network of Scientific Journals from Latin America, the Caribbean, Spain and Portugal

Non-profit academic project, developed under the open access initiative

A real-time colour and image processing p-i-n/p-i-n device with optical readout

M. Vieira, M. Fernandes, P. Louro, and A. Fantoni
Electronics Telecommunication and Computer Dept. ISEL,
R. Conselheiro Emídio Navarro, 1949-014 Lisboa, Portugal,
Tel: +351 21 8317290, Fax: +351 21 8317114,
e-mail: mv@isel.ipl.pt

G. Lavareda and C.N. Carvalho
CFM-UTL-Av. Rovisco Pais, Lisbon

Y. Vygranenko
Univ. of Waterloo, Canada

Recibido el 27 de octubre de 2004; aceptado el 25 de mayo de 2005

A two-terminal, optically addressed image processing device based on two stacked sensing/switching p-i-n a-SiC:H diodes is presented. The charge packets are injected optically into the p-i-n sensing photodiode and confined at the illuminated regions, locally changing the electrical field profile across the p-i-n switching diode. A red scanner is used for charge readout. The various design parameters and addressing architecture tradeoffs are discussed. The influence on the transfer functions of an a-SiC:H sensing absorber, optimized for red transmittance and blue collection or of a floating anode in-between, is analysed. Results show that the thin a-SiC:H sensing absorber confines the readout to the switching diode and light filters the structure, allowing full colour detection at two appropriated voltages. When the floating anode is used the spectral response broadens, allowing B&W image recognition with improved light-to-dark sensitivity. A physical model supports the image and colour recognition process.

Keywords: Optical sensors; image and color recognition; optical readout; tandem devices.

En este trabajo se analizan dispositivos ópticos y de procesamiento de imagen (OSIP) depositados a baja temperatura por PE-CVD en una gran área (4×4 cm²). El dispositivo OSIP consiste en dos diodos apilados (p(SiC:H)/i(Si:H)/n(SiC:H)), con o sin una capa bloqueadora entre ellos, y dos contactos semitransparentes. Para realizar la lectura de carga, se utiliza un sistema de barrido óptico.

El punto principal de este trabajo se centra en la análisis de las características ópticas, en específico la utilización de una parilla metálica (290×290 μm^2 Cr pixels con 40 μm espaciado) entre los dos diodos para actuar como un filtro de luz o como ánodo flotante a través de una capa aislante de a-SiN. La influencia en las funciones de transferencia, resolución, responsividad y tiempo de respuesta del sensor son analizadas. Las características de transferencia óptica-eléctrica revelan una buena eficiencia cuántica, una amplia respuesta espectral, y buena reciprocidad entre la señal de la imagen óptica y eléctrica. Cuando el ánodo flotante está presente, se observa desacoplamiento óptico entre los dos fotodiodos y simultáneamente una buena conductividad eléctrica y una sensibilidad al claro-oscuro aumentada. Son igualmente discutidas la configuración del sensor, el padrón de iluminación y las extensiones de onda del sistema de barrido de modo que se minimiza el enlace cruzado entre los haces de lectura y escrita, incrementando la sensibilidad al claro-oscuro.

Descriptores: Sensores ópticos; reconocimiento de imágenes y color; dispositivos tándem.

PACS: 73.40 Lq; 73.40Ty; 73.40Vz; 73.40Cg

1. Introduction

In our group, large area hydrogenated amorphous silicon single and stacked p-i-n structures with low conductivity doped layers were proposed as Laser Scanned Photodiode (LSP) image sensors [1–3]. These sensors are different from the other electrically scanned image sensors as they are based on only one sensing element with an opto-mechanical readout system. No pixel architecture is needed. Advantages to this approach are large area imaging, high resolution, and uniformity of measurement along the sensor.

This work evaluates the possibility of using two stacked sensing/switching p-i-n photodiodes as a high-sensitivity optically addressed read-write image-processing device (OSIP). A trade-off is established between sensor design and readout parameters. Here, the scanning and the acquisition processes are optimized in order to obtain a full colour image repre-

sentation. The effect of the applied voltage on the colour selectivity and image intensity is discussed and supported by a physical model.

2. Experimental details

The sensing element consists of two stacked p(SiC:H)/i(Si_xC_{1-x}:H)/n(SiC:H)//p(SiC:H)/i(Si:H)/n(Si:H) sensing-switching photodiodes and two transparent conductive oxide (TCO) contacts. The intrinsic and doped layers were fabricated by Plasma Enhanced Chemical Vapour Deposition at 13.56 MHz radio frequency and the transparent contacts by thermal evaporation. In order to decrease the lateral currents that could lead to image smearing, the doped layers (around 200 Å thick) were fabricated by introducing methane during the deposition process [4]. Two configurations are proposed and depicted in Figs. 1a and 1b.

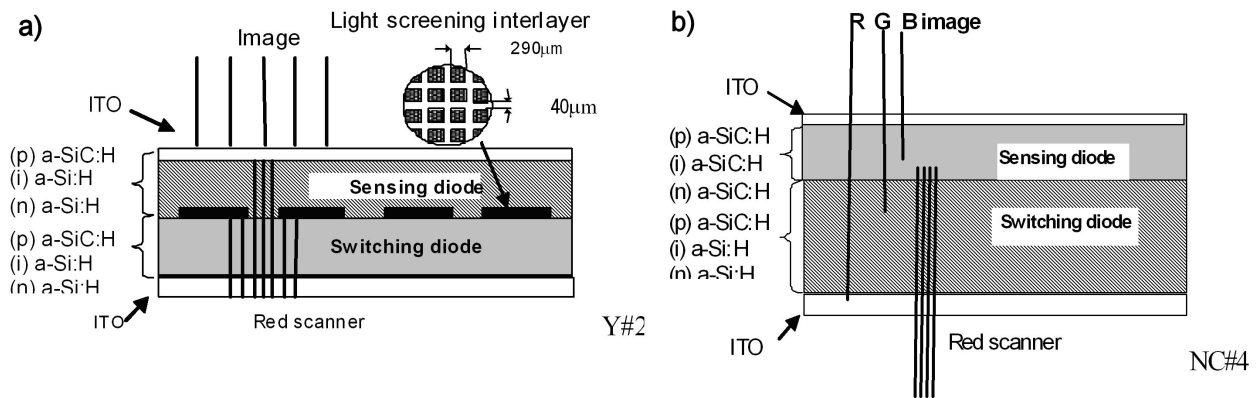


FIGURE 1. Schematic drawing of the optically addressed device: a) optimized for B&W readout and b) optimized for colour recognition.

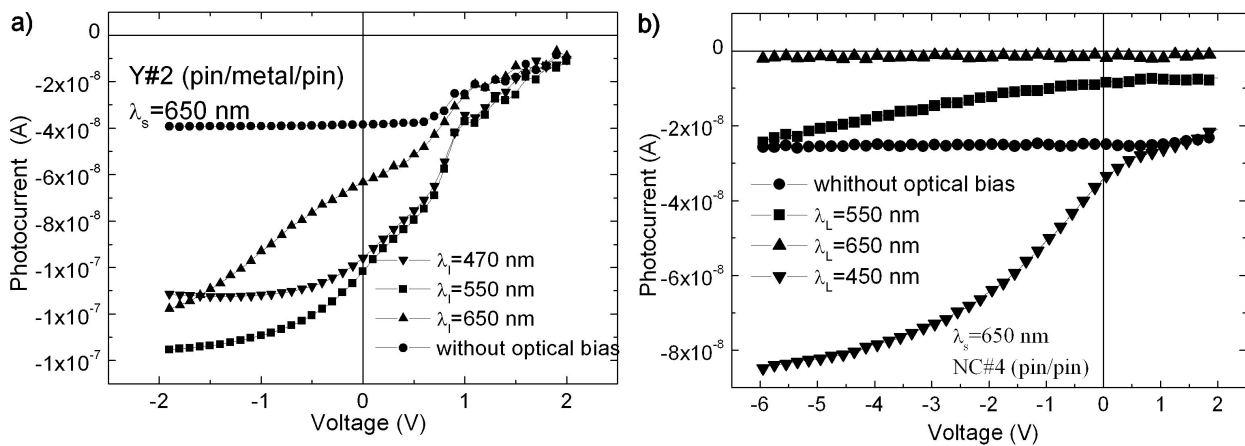


FIGURE 2. Photocurrent as a function of the applied bias (in dark and under blue, green and red irradiation, $\Phi_L=2\text{mW/cm}^2$): a) p-i(a-Si:H)-n /Cr/p-i(a-Si:H)-n and b) p-i(a-SiC:H)-n /p-i(a-Si:H)-n.

The first one (Y#2) is optimized for black and white image readout. Here a 90 nm thermally evaporated Cr light-screening interlayer, composed of $290 \times 290 \mu\text{m}^2$ pixels with 40 μm spacing, was included in order to prevent most (90%) of the light impinging on the switching diode from reaching the sensing one [4], allowing the optical decoupling of both photodiodes. In the second configuration, full colour detection is attempted (NC#4) based on spatially separated absorption of different wavelengths. In order to maximize the blue sensitivity and the red transmittance, an a-SiC:H intrinsic layer (2000 Å) with a band-gap of approximately 2 eV was used as the sensing absorber. Its thickness is a trade-off between sensitivity to the blue/green light and transparency to red photons. The conversion efficiency in the red is maximized by using a 5000 Å thick a-SiH absorber layer at the rear photodiode that works simultaneously as sensing and switching photodiode in the red spectral range. The devices were characterized through the analysis of the photocurrent and spectral response under different steady state optical bias and applied voltages.

The imaging is performed in a write-read simultaneous process: the write exposure, which converts the optical image to a localized packet of charges and the optical read which performs the charge to current conversion by detecting the

photocurrent generated by a light beam scanner. The image and the scanner are incident on opposite sides, as shown in Fig. 1. This approach simplifies the optical system as image and scanner have different optical paths. A low power solid state green laser ($\lambda_{sg} = 550 \text{ nm}$; $\Phi_s = 200 \mu\text{W/cm}^2$) is used as scanner. The scanning beam position is controlled by a two axis deflection system. The line scan speed is close to 1 kHz. Two additional photodiodes provide the synchronization signals for the scanner position information needed for real-time image reconstruction.

3. Results and discussion

In both configurations, in order to optimize the readout parameters and to evaluate the sensors' responsivity to different light pattern wavelengths, the photocurrent generated by the scanner ($\lambda_s = 650 \text{ nm}$) was measured with a lock-in amplifier under different steady-state illumination condition bias ($\lambda_L = 650 \text{ nm}$; 550 nm; 450 nm; $\Phi_L = 200 \mu\text{W/cm}^2$) and displayed in Fig. 2. The sensor element was uniformly illuminated through the back diode (switching diode) with red light, and the optical bias was applied through the front diode side as reported in Fig. 1.

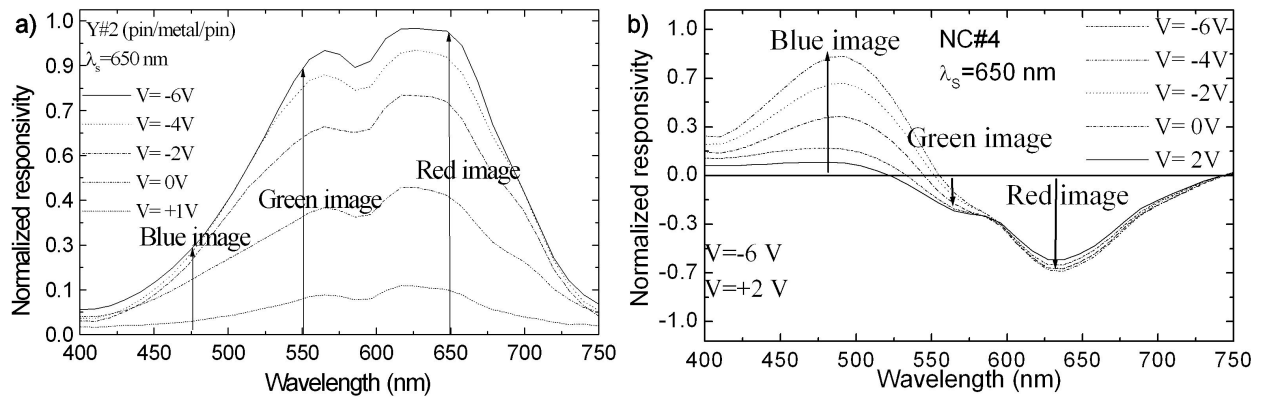


FIGURE 3. a) Normalized responsivity at different electrical bias and acquired images at three different colours: Y#2 (a) and NC#4 (b).

Results show that under reverse bias, the red scanner responsivity, in the absence of an optical bias, is almost independent of the applied voltage, while under green/red irradiation it is enhanced when a metal screen interlayer is used (Fig. 2a) or reduced in its absence (Fig. 2b). For both sensors, the responsivity under blue irradiation (absorbed exclusively inside the sensing diode) presents the same trend. When a metal screening layer is used for optical decoupling (Fig. 2a), the increased responsivity of the switching diode, under reverse bias and green/red illumination, can be explained through the self-biasing concept. Since the current across the structures has to be the same, the irradiated sensing diode, acting as a load, converts the light bias into an electric field (proportional to the light intensity) across the switching diode that becomes reverse biased and switches to its OFF state, becoming sensitive to the incoming scanner light. Without optical bias, the front diode is not conducting and ideally the voltage drop across the bottom one is not enough to switch it to its OFF state (full depletion), decreasing the collection of the photogenerated carriers by the scanner [5]. When the light (green/blue) is absorbed inside the sensing diode (5000 \AA), the switching diode becomes fully depleted and so the current generated by the scanner becomes independent of the applied voltage. Under red irradiation, and due to the transparency of this 20-30 nm Cr interlayer, the portion of light absorbed into the switching diode reduces its depletion region, pushing the switching diode to its ON state (load). Thus, the linear decrease of the photocurrent with the applied voltage corresponds to a decrease in the depletion depth inside the switching diode.

A different behaviour of the photocurrent is observed (Fig. 2b) when, instead of a light screen layer for optical decoupling (Fig. 1a), a thin a-SiC:H intrinsic layer is used (Fig. 1b) to produce the separation of the spectrum into bands. Its thickness and the optical gap (2000 \AA , 2 eV) were optimized for high conversation efficiency in the blue light and transparency of the red photons coming either from the image or from the scanner. The green photon absorption occurs across the sensing diode, the n-p defectuous interface, and at the front side of the switching diode (Fig. 1b). Under reverse bias and blue irradiation, the collection is high

since the switching diode becomes fully depleted due to its self-biasing process. Under red illumination, due to the high light penetration depth of the red photons and higher conversion efficiency of the a-Si:H switching absorber acting as a load (ON state), the collection is almost non-existent. In the green spectral range, as the reverse bias increases due to the increase of the potential drop across the switching diode, the collection increases linearly. It is interesting to note that around -6 V , the collection with or without green optical image are the same, leading to the rejection of green images.

In order to evaluate the sensors' responsivity to different light pattern wavelengths, the photocurrent generated by the scanner ($\lambda_s = 650 \text{ nm}$, $10 \mu\text{Wcm}^{-2}$) was measured under different steady-state illumination conditions ($400 \text{ nm} < \lambda_L < 750 \text{ nm}$, $\Phi_L = 100 \mu\text{Wcm}^{-2}$). The normalized image intensities are displayed in Fig. 3a for sensor Y#2 and in Fig. 3b for the sensor NC#4, under different values of electrical bias ($-6 \text{ V} < V < 2 \text{ V}$). Also shown are the acquired images of the same green, red and blue pictures (5) projected, one by one, on the active surface of the sensing diode and acquired through the switching diode side with a red scanner. The line scan frequency was close to 1 kHz , and no algorithms were used during the image restoration process. Assuming the readout time of 1 ms , then the frame time for a 50-line image is around 50 ms .

Results show that the internal Cr light-screening metal layer prevents the light from the optical image from reaching the switching diode, making an effective optical decoupling possible between both diodes and also a good electrical conductivity via the metal grid that also acts as a floating node, forcing the self reverse biasing of the switching diode and allowing a better collection of the carriers generated by the scanner. During the image acquisition process, beneath the dark regions, the electrical field across the rear diode is low. The collected current stays at its minimum value (dark level), resulting in a weak image signal (black regions). At the illuminated regions, as the incoming light is entirely absorbed into the sensing diode (green/red), the electrical field in the absorber is enhanced (proportionally to the light intensity) and the collection of the carriers generated by the red scanner increased. The result is an increased image signal

(white regions). As expected from Figs. 2a and 3a, no colour discrimination is possible. Nevertheless, a black and white image was acquired with improved resolution ($50\ \mu\text{m}$) and contrast at a continuous and fast readout.

For sensor NC#4, the responsivity in the red spectral region (Fig. 3b) is strongly influenced by the lack of the metal light screening inter-layer. Without this layer, the collection efficiency is enhanced in the blue region, decreases abruptly in the green range and, in the red region, becomes negative relative to the dark value, leading to a negative image due to the optical mismatch between the optical image and the optical scanner. As the applied bias changes from forward to reverse, the image contrast increases. Results show that the image signal is positive in the blue range almost negligible in the green region, and negative in the red range (see arrows in Fig. 3). By tuning the voltage to $-6\ \text{V}$, the red and blue signal are high and opposite in sign and the green signal is suppressed, allowing blue and red colour recognitions. The green information is obtained under slight forward bias, where the blue signal goes down to zero. Combining the information obtained at three applied voltages, a RGB colour image can be acquired with this two terminal wavelength optimized sensor without the need of the usual colour filters.

4. Conclusions

Two wavelength-optimized optical signals and an imaging device for B&W and colour image recognition were presented. A trade-off between sensor configuration and readout parameters was established in order to improve the resolution and the contrast of the image.

The metal light-screening layer proved to be effective to optically decouple the scanner from the image, giving a fast B&W image with increased resolution. For colour recognition, a thin a-SiC:H sensing absorber was needed. By sampling the absorption region at different bias voltages, it was possible to extract separately the RGB integrated information with a good rejection ratio. In both sensors a readout of 1000 lines per second was achieved allowing continuous and fast image sensing, and colour recognition on sensor NC#4.

Acknowledgements

This work has been financially supported by IPL project n°13-2003.

-
1. M. Vieira *et al.*, *IEEE Sensor Journal* **1** (2001) 158.
 2. M. Vieira, M. Fernandes, P. Louro, R. Schwarz, and M. Schubert, *J. Non Cryst. Solids* **299-302** (2002) 1245.
 3. M. Vieira, A. Fantoni, M. Fernandes, P. Louro, and I. Rodrigues, *Mat. Res. Soc. Symp. Proc* **762** (2003) A.18.13.
 4. M. Fernandes, M. Vieira, I. Rodrigues, and R. Martins, *Sensors and Actuators A physical* (2004) 360.
 5. M. Vieira, M. Fernandes, P. Louro, A. Fantoni, and R. Schwarz, *J. Non Cryst. Solids* **338-340** (2004) 754.